

The Running Coupling From Lattice QCD¹

Gunnar S. Bali²

Fachbereich Physik, Bergische Universität, Gesamthochschule Wuppertal
Gaußstraße 20, 42097 Wuppertal, Germany

ABSTRACT

A recent lattice calculation of the QCD running coupling is presented. The coupling is extracted from the force between two static quarks in the framework of the valence quark approximation. A value of the Λ -parameter for zero quark flavours is determined: $\Lambda_{\overline{MS}}^{(0)} = 0.630(38)\sqrt{\sigma} = 293(18)^{+25}_{-63}$ MeV. The first error is statistical, the second stems from the overall scale uncertainty in the string tension σ . Combining this value with results from full QCD lattice simulations, we end up with the estimate $\Lambda_{\overline{MS}}^{(4)} = 129(8)^{+43}_{-60}$ MeV or $\alpha_{\overline{MS}}(m_Z) = 0.102^{+06}_{-11}$.

¹Talk presented at the XVI Workshop on High Energy Physics, Sept. 14–17 1993, Protvino, Russia.

²E-mail: bali@wpts0.physik.uni-wuppertal.de

1 Introduction

QCD, the theory of strong interactions, contains 8 free parameters, namely the quark masses, a (\mathcal{CP} -violating) vacuum angle Θ which is consistent with *zero*, and the running coupling parameter, that can only be fixed by experiment. For an empirical test of QCD, the following four steps have to be performed:

1. measurement of 8 independent observables (e.g. particle masses),
2. fixing the free parameters by use of QCD,
3. predicting a value for another observable,
4. comparison with experiment.

It turns out that the second step is highly non trivial. So, most of this talk will deal with this task. I will use experimental data on the mass of the ρ -meson m_ρ , and the string tension σ , obtained from the quarkonia spectra, in order to predict the running of the coupling from QCD, which can then be compared to experiment. Since the precision of the lattice determination of α_S can compete with the experimental *status quo*, the result can be used as an input for phenomenological calculations.

There are different ways to define a running coupling. Either one can state a value for $\alpha_S(\mu)$ at some fixed scale μ (like the mass of the Z^0 boson m_Z), the momentum μ , at which the coupling has a given strength, or a Λ -parameter from the functional dependence $\alpha(q) = f(q/\Lambda)$, which can be obtained in perturbation theory, for high momenta transfer q . Here, I take a low energy scale μ , and calculate $\alpha_S(N \times \mu)$ on the lattice with N being a large number, in order to make contact with energies at which perturbation theory becomes valid. It is in this region where one can translate one scheme into another.

The only known method which allows to treat QCD problems

- nonperturbatively,
- quantitatively,
- from first principles, and
- with control over possible systematic errors,

is Lattice Gauge Theory. Unfortunately, it is a stochastical (non-exact) method, and thus statistical errors are introduced. Also, computational resources are a serious limitation. Since speed of supercomputers evolves according to an exponential scaling law in time, the latter problem seems to vanish. In the following, I will give a brief methodological introduction into lattice gauge theory, and comment on the advantages and caveats. This is followed by a section about how to determine the physical spacing of a given lattice,

a section about improved perturbation theory on the lattice, and a section about our actual calculation of α_S from the interquark force, and how to relate the result obtained to schemes which are more commonly used in perturbative QCD. At the end an outlook is given.

2 Lattice Gauge Theory

The first step in introducing the lattice formulation of a gauge theory is a rotation from Minkowski to Euclidean space ($t \rightarrow it$). Because of this rotation, information about real time dynamics is lost but static quantities like the mass spectrum remain unharmed. Then, space-time is approximated by a four dimensional hypercubic lattice with spacing a and extent La . π/a serves as the required ultraviolet cutoff. After this is done, calculations of quantities of interest on the lattice are performed. Since a stochastic (Monte-Carlo) method is used, one also describes this procedure with the term “measurements are taken”. Finally, the results are translated back to the continuum. For this step, various extrapolations become necessary. The limit $a \rightarrow 0$ (that corresponds to the limit $g^2 \rightarrow 0$ in asymptotically free theories) can be calculated by use of ordinary perturbation theory in the coupling parameter g^2 , once the perturbative region is reached. The infinite volume limit $La \rightarrow \infty$ can be reached by use of Finite Size Scaling methods which are well established in statistical mechanics, and the extrapolation to small quark masses is controlled by chiral perturbation theory.

In the following, I will briefly describe some basic notations, used in lattice QCD. The Wick-rotated action $S_{QCD} = S_g + S_f$ contains a purely gluonic part, S_g , which can be written as

$$S_g = -\frac{1}{4} \int d^4x F_{\mu\nu}^a F_{\mu\nu}^a = -\beta \underbrace{\sum_{n,\mu>\nu} \left(1 - \frac{1}{N} \text{Re} \text{Tr}\{U_{\mu\nu}(n)\} \right)}_{S_W} + \mathcal{O}(a^2) \quad (1)$$

with $\beta = 2N/g^2$, and the number of colours $N = 3$. g^2 is the bare lattice coupling. The discretized version of the gluonic action, S_W , is the so-called Wilson action. The continuum four-vector x is mapped to the discrete vector $n = x/a$. Instead of non-compact gauge fields, $A_\mu(x)$, $SU(3)$ matrices are introduced:

$$U_\mu(n) = \mathcal{P} \left[\exp \left(ig \int_{na}^{n(a+\hat{\mu})} dx A_\mu(x) \right) \right] \quad . \quad (2)$$

In terms of these, the gauge symmetry is easier to preserve since products of such “link-variables” along a closed path, e.g. the Wilson action, are automatically gauge invariant. The lattice version of the Maxwell field strength tensor, then, is the ordered product of link variables around an elementary square (plaquette) $U_{\mu\nu}(n) = \exp(iga^2(F_{\mu\nu}(an) + \mathcal{O}(a)))$. In the following it will also be referred to as U_\square .

Expectation values of observables O are calculated in the path integral approach as

their mean value over all possible field configurations in the finite box

$$\langle O \rangle = \frac{1}{Z} \int \left(\prod_{n,\mu} dU_\mu(n) \right) O e^{-\beta S_W} \quad , \quad Z = \int \left(\prod_{n,\mu} dU_\mu(n) \right) e^{-\beta S_W} \quad . \quad (3)$$

In order to solve this high dimensional integral, N independent field configurations $C_i = \{U_\mu^{(i)}(n)\}$ are generated according to the measure $dP(C_i) = \left(\prod_{n,\mu} dU_\mu^{(i)}(n) \right) e^{-\beta S_W(C_i)}$. The expectation value is calculated on a “representative ensemble”

$$\langle O \rangle = \lim_{N \rightarrow \infty} \frac{1}{N} \sum_{i=1}^N O(C_i) \quad . \quad (4)$$

This gives rise to a statistical error, ΔO , which reduces as N is increased: $\Delta O \propto 1/\sqrt{N}$.

In the present calculation, the valence quark (quenched) approximation ($S_f = \text{const.}$) is used, in which vacuum polarization effects, caused by sea quarks, are neglected. In the language of perturbation theory this means that fermionic loops are dropped while gluonic diagrams are taken to all orders. The reason for this approximation are limited computational resources. However, all mass ratios from real world experiments are reproduced within an error of 6% [1]. So, if full QCD with its dynamical fermions describes nature, discrepancies between full and quenched results are likely to coincide within 10% or so. This claim is also supported by the success of simple models like the naive quark model.

3 How to set the mass scale

In quenched lattice QCD, the inverse bare coupling β is the only free external parameter. So, the value of β determines the masss scale (and lattice spacing a): One measures a physical mass M in lattice units, and fixes the lattice spacing by the corresponding experimental value m_{phys} : $a(\beta) = m_{\text{phys}}/M(\beta)$. On repeating this procedure for various β one can determine the dependence of the spacing on the bare coupling $a(g^2)$, or, by inverting this relation, extract a running coupling $g^2(a)$. As soon as a behaviour according to perturbation theory is observed (asymptotic scaling), this running lattice coupling can be translated into any other renormalization scheme perturbatively.

The present simulations have been performed at the β values $\beta = 5.5, 5.6, 5.7, 5.8, 5.9, 6.0, 6.2, 6.4$ and 6.8 . $L = 16$ was chosen for the first five values, and $L = 32$ for the latter four. Below $\beta = 5.5$ ($a \approx 0.25$ fm) agreement with strong coupling expectations is found. Between 5.5 and 5.7 ($a \approx 0.18$ fm), as the (largest) correlation length in lattice units increases up to a few lattice spacings, a transition from discrete hypercubic symmetry to continuum rotational symmetry $\left(\sum_i |R_i| \longrightarrow \sqrt{\sum_i R_i^2} \right)$ is observed on the scale of a few a . Between 5.7 and 6.0 ($a \approx 0.1$ fm) ratios of physical masses, extracted from the lattice, remain constant within about 10%. From 6.0 up to 6.8 ($a \approx 0.03$ fm), these ratios remain constant within statistical accuracy of contemporary lattice simulations.

This is referred to as scaling in contrast to asymptotic scaling that does not set in for $\beta < \mathcal{O}(10)$ at least.

In order to fix the physical mass scale, we use the string tension $\sigma = K/a^2$ which is defined to be the slope of the potential between heavy quark sources $V(R)$ at large $q\bar{q}$ -separations

$$K = -\lim_{R \rightarrow \infty} F(R) \quad , \quad F(R) = -\frac{\partial V(R)}{\partial R} \quad . \quad (5)$$

The obvious advantages in extracting the mass scale from the potential can be summarized as follows:

- The measurement of $V(R)$ consumes little computer time since no matrices have to be inverted for calculation of propagators.
- Finite size effects are negligible for $La > 1$ fm [2, 3].
- No extrapolations in the quark masses are needed.
- The string tension is the most accurately measured dimensionful quantity on the lattice [4, 5].

In the following I will discuss, which physical scale corresponds to $\sqrt{\sigma}$ and how to define it reasonably on a lattice with finite extent.

Apart from investigations of Regge trajectories which suggest values $\sqrt{\sigma} \approx 400\text{--}450$ MeV, potential related information can be gained from the Charmonium and Bottomonium spectra by integration of the Schrödinger equation [7, 8, 9]. It is practically only the potential at distances r between about 0.2 fm and 1 fm that determines these quarkonia spectra, since the corresponding wavefunctions almost vanish for smaller or larger $q\bar{q}$ separations. This is a lucky incidence because for smaller r relativistic corrections to the Schrödinger equation would have to be taken into account. For larger separations ($r > 1$ fm), differences between the quenched potential (without sea quarks) and the real QCD potential are expected due to creation of a $q\bar{q}$ pair from the vacuum (string breaking). The phenomenological potential is well described by the Cornell parametrization

$$V(R) = V_0 - \frac{e}{R} + KR \quad . \quad (6)$$

Before discovery of the Υ' , typical fit parameters have been $\sqrt{\sigma} = 455$ MeV, and $e = 0.25$ [7]. After inclusion of the Υ mass splitting, these parameters moved rapidly to values like $\sqrt{\sigma}=412$ MeV, $e = 0.51$ [8] or $\sqrt{\sigma}=427$ MeV, $e = 0.52$ [9]. A careful inspection shows that the $e \approx 0.25$ and $e \approx 0.5$ parametrizations of the potential differ only weakly within the accessible range (0.2 to 1 fm). This is related to the fact that the fit parameters are highly correlated.

We have attempted to fit our lattice potential (Fig. 1) for a fixed physical cutoff $Ra \geq 0.3$ fm³, and different β to the Cornell form. In Fig. 2a we display the scatter of

³For $\beta = 5.5$ and $\beta = 5.6$, $Ra \geq 0.5$ fm, $Ra \geq 0.4$ fm have been chosen, respectively.

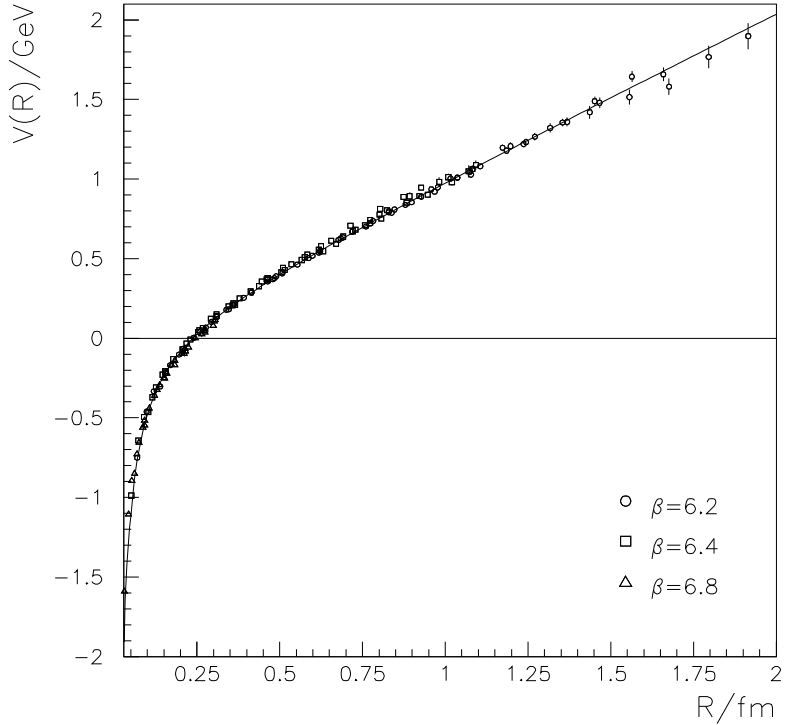


Figure 1: *The (quenched) QCD potential $V(R)$, measured at $\beta = 6.2$, $\beta = 6.4$, and $\beta = 6.8$ as a function of r in physical units. The mass scale is extracted from the string tension.*

fit parameters among different bootstrap samples in the K - e -plane where we observe a correlation, similar to the ambiguity in parametrizing the quarkonium potential. To circumvent this problem, Sommer has invented a more stable scale from the potential [10] that is also well-defined in the screened case of full QCD. The idea is to calculate the dimensionless quantity $X(R_0) = -F(R_0)R_0^2$ from the interquark force. Since the potential models are most sensitive to the spectrum at a distance of about 0.5 fm, a scale $r_0 = R_0 a \approx 0.5$ fm is defined by imposing the condition $X(R_0) = 1.65$. Using the fit parameters of Ref. [7] one ends up with $r_0^{-1} = 384$ MeV. Ref. [8] yields $r_0^{-1} = 386$ MeV and Ref. [9] $r_0^{-1} = 402$ MeV. Another set of fit parameters, taken from Ref. [9], leads to $r_0^{-1} = 416$ MeV. We conclude with the value $r_0^{-1} = (400 \pm 15)$ MeV.

Deviating from Sommer's prescription, we fit the potential to the Cornell ansatz and calculate

$$R_0^{-1} = \sqrt{\frac{K}{1.65 - e}} \quad (7)$$

from the fitted parameters. All fits yield effective Coulomb coefficients consistent with the value $e = 0.296$, determined from the $\beta = 6.2$ data that carries the smallest errors. For convenience, we rescale the value of r_0^{-1} by the factor $\sqrt{1.65 - 0.296} = 1.164$ in order to obtain a string tension $\sigma_r = 1.164r_0^{-1}$. A bootstrap scatter plot in the K - e -plane is displayed in Fig. 2b. It can be seen that this definition of a string tension is insensitive

Figure 2: *The fit parameter e versus $K^{1/2}$ (Eq. 6), and the redefined string tension, calculated from R_0^{-1} (Eq. 7). The distribution of 1000 bootstrap samples is shown. The higher the density of the points, the larger is the corresponding probability.*

towards the value of the Coulomb coefficient e . The string tension results are summarized in Tab. 1. A detailed description of the data evaluation and fitting procedures will be given elsewhere [6]. The physical value that corresponds to the redefined string tension is

$$\sigma_r = 465 \pm 18 \text{ MeV} \quad . \quad (8)$$

While ratios of pure glue quantities like the 0^{++} or 2^{++} glueball masses in units of the string tension exhibit good scaling behaviour above $\beta = 5.7$ [11], the situation concerning observables with valence quark content is less satisfactory at present values of β . In order to take these effects into account we have extrapolated our string tension

β	S_{\square}	$\sqrt{\sigma_r}a$
5.5	0.503196(18)	0.5805(84)
5.6	0.475495(27)	0.5092(136)
5.7	0.450805(25)	0.4069(78)
5.8	0.432349(21)	0.3206(41)
5.9	0.418164(15)	0.2518(62)
6.0	0.406318(5)	0.2204(17)
6.2	0.386369(3)	0.1582(9)
6.4	0.369364(2)	0.1179(9)
6.8	0.340782(4)	0.0698(18)

Table 1: *The average plaquette action, and the redefined string tension in lattice units.*

values to $\beta = 5.93$ and $\beta = 6.17$, using the E -scheme that will be described below, and calculated the ratio of the ρ mass, taken from Ref. [1], over the string tension at these β -values and at $\beta = 5.7$. After this, linear and quadratic fits on the a dependence of this ratio have been performed, yielding a continuum value of $2 > m_\rho/\sqrt{\sigma} > 1.7$. This corresponds to $385 \text{ MeV} < \sqrt{\sigma} < 455 \text{ MeV}$. The difference between this range and the number from the potential analysis (Eq. 8) might be caused by both, scaling violations still present above $\beta = 6.0$, and quenching. If we take this uncertainty into account and allow for an additional 5% quenching error, we end up with the conservative scale estimate

$$\sigma_r = 465_{-100}^{+40} \text{ MeV} . \quad (9)$$

By full QCD simulations the huge systematic error can probably be reduced to about 5% or even less. In the following, σ_r will be abbreviated as σ , and $\sigma_r a^2$ as K .

4 Asymptotic scaling and redefined couplings

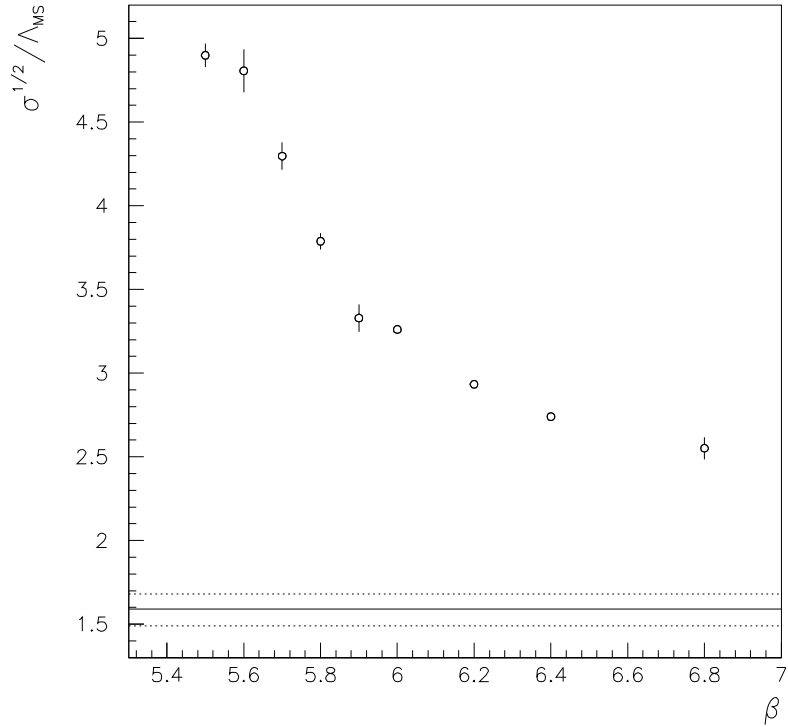


Figure 3: The ratio $y = \sigma^{1/2} / \Lambda_{\overline{\text{MS}}}$ in the two-loop approximation, calculated by use of the bare coupling $g^2 = 6/\beta$. The error band denotes the value $y = 1.59 \pm 0.10$, extracted from the running of the coupling $\alpha_{q\bar{q}}$ from the interquark force.

The QCD β -function can be expanded perturbatively

$$-\frac{\partial g^2}{\partial \ln a} = -b_0 g^3 - b_1 g^5 + \dots . \quad (10)$$

Higher order terms are regularization scheme and gauge dependent. The first two coefficients are given by:

$$b_0 = \frac{11N - 2n_f}{3(16\pi^2)} \quad , \quad b_1 = \frac{34N^3 - (13N^2 - 3)n_f}{3N(16\pi^2)^2} \quad . \quad (11)$$

n_f denotes the number of quark flavours, N the number of colours. Integrating this β -function leads to

$$a\Lambda_L = f(g^2) := e^{-1/2b_0g^2} (b_0g^2)^{-b_1/2b_0^2} \quad , \quad (12)$$

where Λ_L is an integration constant, not predicted by the theory. For sufficiently small g^2 , the ratio $\sqrt{\sigma}/\Lambda_L = \sqrt{K}/a\Lambda_L = \sqrt{K}/f(g^2)$ is expected to remain constant. This perturbative behaviour is called “asymptotic scaling”. As can be seen from Fig. 3 there are large deviations from the asymptotic expression for $\beta < 7$. On the other hand it is the β region $\beta > 6$ where good scaling between physical quantities like mass ratios is observed. So it might be that just the bare coupling is an ill behaved expansion parameter [12]. The situation might be improved if one chooses a more appropriate renormalisation scheme by use of a more “physical” coupling parameter.

Several suggestions have been made in the past for “better” couplings. I will review three such choices which have been proven to be successful, at least in the β range accessible to present day computer simulations. All are based on the idea of mean field improvement and were stimulated by Parisi [13]. The Fermilab group proposed an improved coupling g_{FNAL}^2 [14, 15] which corresponds to the continuum modified minimal subtraction (\overline{MS}) scheme [16] in the limit $a \rightarrow 0$. A perturbative calculation [17] shows

$$\frac{1}{g_{\overline{MS}}^2(\mu)} = \frac{1}{g^2(\mu)} \underbrace{-d + 0.008204N + 0.00278n_f + \dots}_{\Delta} \quad , \quad d = \frac{N^2 - 1}{8N} \quad . \quad (13)$$

The large correction coefficient d , caused by tadpole diagrams, leads to the relation $\Lambda_{\overline{MS}} = \pi e^{-\Delta/2b_0} \Lambda_L = 28.81 \Lambda_L$ for $N = 3$, $n_f = 0$. On the lattice, the average plaquette action $\langle S_{\square} \rangle = \langle 1 - U_{\square} \rangle$ can be expanded in powers of g^2 [18, 19, 20]

$$\langle S_{\square} \rangle = c_1 g^2 + c_2 g^4 + c_3 g^6 + \dots \quad . \quad (14)$$

The fields $A_{\mu}(x)$ are expected to fluctuate around *zero*. So the mean field action is expected to be *zero*. Since the coefficient c_1 , that causes the deviations from this expectation, turns out to equal the large number d , that has been responsible for the huge difference between the two Λ -parameters, the idea is to substitute $d = c_1$ by $\langle S_{\square} \rangle/g^2$. This leads to the redefined coupling

$$\frac{1}{g_{\text{FNAL}}^2(\pi/a)} = \frac{\langle U_{\square} \rangle}{g^2(\pi/a)} + 0.008204N + 0.00278n_f \quad (15)$$

with $\Lambda_{\text{FNAL}} = \Lambda_{\overline{MS}}$. In Ref. [15] a different scheme is introduced, in which a coupling g_V^2 is defined from logarithms of small Wilson loops.

Another empirical concept is the *E*-scheme, proposed in Ref. [21]. The starting point is the observation that large deviations from asymptotic scaling exist as well as

many quantities like the average plaquette are not well described by perturbation theory. The idea, now, is that the contributions, polluting the perturbative expansion of the plaquette, might be similar to those spoiling asymptotic scaling. By defining a coupling from inverting Eq. 14, one forces the plaquette to behave according to perturbation theory, and hopes to find asymptotic scaling for dimensionful quantities as well. The E coupling is defined by $g_E^2 = \langle S_{\square} \rangle / c_1$ with $\Lambda_E = e^{c_2/(2c_1b_0)} \Lambda_L = 2.0756 \Lambda_L$ for $N = 3$, $n_f = 0$. Another suggestion [4, 22] to define a g_{E2}^2 by inverting Eq. 14 after the second order. Then $\Lambda_{E2} = \Lambda_L$.

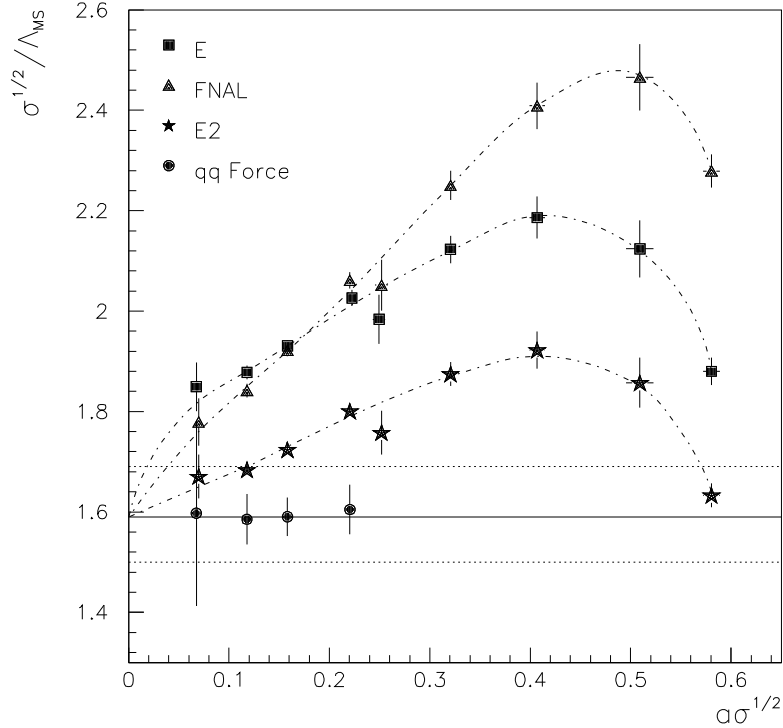


Figure 4: The ratio $y = \sigma^{1/2} / \Lambda_{\overline{MS}}$ in the two-loop approximation, calculated by use of the improved couplings versus the lattice spacing. The error band denotes the value $y = 1.59 \pm 0.10$, extracted from the running of the coupling $\alpha_{q\bar{q}}$ from the interquark force (circles). The curves are just drawn to guide the eye.

In Fig. 4 the effective $\Lambda_{\overline{MS}}^{-1}$, obtained by use of the two-loop β -function is plotted in units of the string tension versus the lattice spacing a for the above three effective couplings. We find that the behaviour is improved in all cases, though the E -schemes appear to be more stable than the FNAL- \overline{MS} -scheme. The differences between the values, obtained from the effective schemes reflect still present deviations from asymptotic scaling. One might attempt to extrapolate $\sqrt{\sigma} / \Lambda_{\overline{MS}}$ to $a = 0$. If the corrections to the two-loop formula Eq. 12 can be resummed into an effective third order perturbative coefficient one might attempt to fit the data to the parametrization

$$y(a(g^2)) = y(0) \left(1 - \mathcal{O}(g^2) \right) = y(0) \left(1 + \frac{C}{\ln(y(0)/(a\sqrt{\sigma}))} \right) , \quad y(a) := \frac{\sqrt{\sigma}}{\Lambda_{\overline{MS}}(a)} \quad (16)$$

where $y(0)$ and C are fit parameters.

Another possibility that works equally well is to argue that the deviations are of nonperturbative origin and might be parametrized by a polynomial in the lattice spacing a . For $5.7 < \beta \leq 6.8$ the data is well described by a linear fit, although from Eq. 16 it is clear that the behaviour might change rapidly as one approaches the continuum limit. As can be imagined from Fig. 4, with the described variety of fitting opportunities the extrapolated ratio might be anywhere within the range $1.4 < \sqrt{\sigma}/\Lambda_{\overline{MS}}(0) < 1.8$.

5 Direct “measurement” of α_S

So far we have inserted a coupling g^2 (or calculated an effective g^2 at a fixed β), and measured the corresponding scale $a(g^2)$. The effective couplings are also calculated from the plaquette, i.e. on a characteristic length scale a . This might cause nonperturbative deviations from asymptotic scaling that depend on the chosen discretization of the action. In order to reduce these “discretization errors”, one should determine a coupling from observables with a typical scale of a few lattice spacings, instead. So far there have been three such approaches.

1. Extracting couplings from logarithms of small Wilson loops by tadpole-improved perturbation theory [23].
2. Introducing a volume dependent coupling [24] from the field response to the boundary conditions and exploiting finite size matching techniques on small volumes [25].
3. Calculating α from a “physical” quantity like the interquark force [26, 4, 22].

All these methods have their specific merits and disadvantages. Nonetheless, the results are fairly consistent with each other. In the first approach, it is not *a priori* obvious, what effective momentum corresponds to a Wilson loop with a certain extent [15]. Also, one still encounters deviations from asymptotic behaviour that have to be examined carefully by simulating at various β . An obvious advantage of this method is that Wilson loops are amongst the most simple quantities that can be calculated on the lattice. The second approach is a bit awkward since the boundary conditions have to be fixed. Thus, the generated configurations can only be used for the single purpose of calculating the coupling. While in the other two methods, $\alpha(\mu)$ can be computed from one simulation. Since the coupling is defined in a technical way (that allows for an easier perturbative expansion around the fixed background), the coefficient, connecting this scheme to the continuum motivated \overline{MS} scheme, is large, and two-loop perturbative behaviour is only found for rather high energies. At present, it is not clear how this method can be generalized to full QCD with its dynamical fermions. The advantage is that the energy scale can be doubled with much less effort than when using a single-lattice method like approach 3, which I am going to discuss in the following.

The intuitive picture behind the concept of a coupling is that of local interactions. These are only realized at large energies where perturbation theory becomes a valid approximation. In principle, any dimensionless quantity that depends on a mass scale can be called a coupling. In the case of the quenched approximation to QCD, only one such mass scale exists. The β -function, i.e. the logarithmic derivative of the coupling with respect to the mass, is universal up to two loops perturbation theory. Just the renormalization point differs from scheme to scheme. The schemes can be translated into each other by perturbation theory at large energies (small couplings). In the lattice formulation it is possible to define various nonperturbative gauge invariant couplings which can only be connected with each other in this high energy region. So one is forced to use a small lattice spacing, in order to make the results applicable in the framework of perturbation theory. A volume $(La)^3 > 1 \text{ fm}^3$ is needed to minimize finite size effects on the $q\bar{q}$ -potential [2, 3]. Since the computer memory of our machine (an 8K CM-2) is limited to 256 MBytes $L \leq 32$ has to be chosen. These two constraints (the physical and the technical) set the limit $a^{-1} < 6 \text{ GeV}$. Only potential values from $R \geq \sqrt{2}$ are included into the analysis of the interquark force, in order to minimize discretization errors. As a check whether these are eliminated, simulations at different spacings a are needed. Fortunately, clearly perturbative behaviour is found for distances as small as 1 GeV^{-1} , i.e. over a scale factor 3–4 within the accessible energy range.

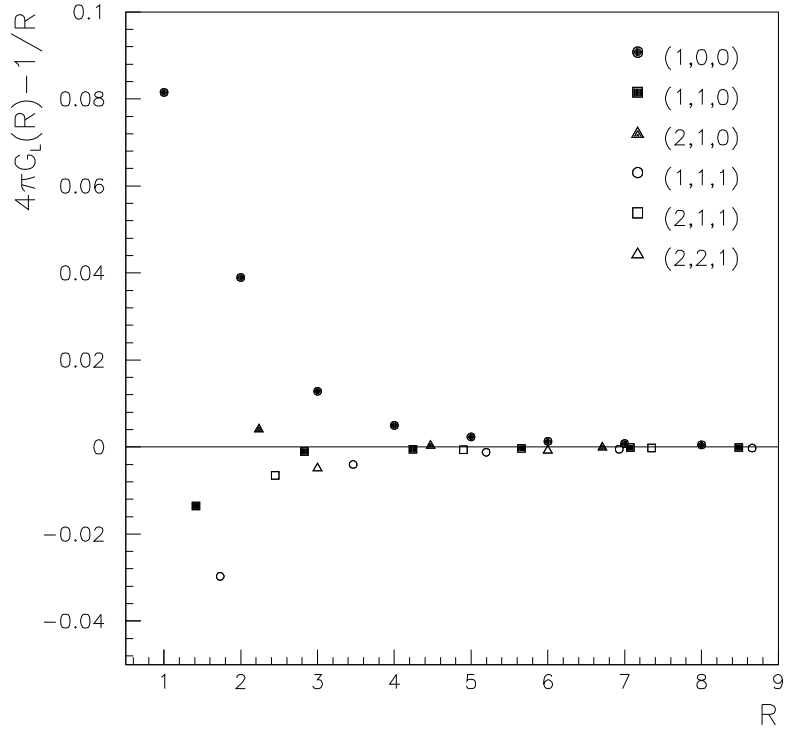


Figure 5: *Difference between the lattice one gluon exchange and the continuum $1/R$.*

In order to increase the energy resolution we have to use information, obtained from $q\bar{q}$ separations where effects of broken continuum $O(3)$ symmetry are still visible. The

corresponding values of the force can be corrected from theoretical knowledge about the nature of these violations. The one gluon exchange, which causes a continuum potential $V_c(\mathbf{R}) \propto -1/R$, is replaced by the Fourier transform of the lattice gluon propagator [27]

$$\frac{1}{R} \longrightarrow \left[\frac{1}{\mathbf{R}} \right] := 4\pi G_L(\mathbf{R}) = 4\pi \int_{-\pi}^{\pi} \frac{d^3 p}{(2\pi)^3} \frac{\cos(\mathbf{R}\mathbf{p})}{4 \sum_i \sin^2(p_i/2)} \quad . \quad (17)$$

In Fig. 5, the difference between the two tree-level results for all $q\bar{q}$ directions, realized in our simulations, is displayed. As can be seen, from $R = 4$ onwards it becomes negligible, and it is largest for the on-axis (1,0,0) separations. The one-loop coefficient has been calculated for the on-axis values only [19], and gives — apart from a renormalization of the bare coupling parameter

$$V(\mathbf{R}) \propto - \left[\frac{1}{\mathbf{R}} \right] \frac{1}{\ln(\Lambda_V(R)R)} \quad . \quad (18)$$

For large lattices and $R > 1$, the deviations of $\Lambda_V(R)$ from the continuum Λ_V are less than 5%, and for the off-axis directions, they are probably even smaller.

Exploiting this knowledge, we will reconstruct the continuum force $F(R)$ and check our procedure by comparing results from four different lattice spacings reaching from 2 GeV to more than 6 GeV. Then, we will define the coupling from the interquark force

$$\alpha_{q\bar{q}}(R) = -\frac{2N}{N^2 - 1} F(R) R^2 \quad . \quad (19)$$

Finally, we calculate $\Lambda_R = 1.048\Lambda_{\overline{MS}}$ [28] from the running of the coupling according to

$$\alpha_{q\bar{q}}(R) = \frac{1}{4\pi} \left(b_0 \ln(R\Lambda_R)^{-2} + b_1/b_0 \ln \ln(R\Lambda_R)^{-2} \right)^{-1}, \quad (20)$$

and translate our result into the \overline{MS} scheme: $\alpha_{\overline{MS}}(q) = \alpha_{q\bar{q}}(r) - 0.082\alpha_{q\bar{q}}^2(r) + \dots$ with $r = 1/q$. It is this small two-loop coefficient (0.082), and the dependence on just a single parameter (Λ_R), which turn the interquark force $F(R)$ into a more user-friendly quantity than the potential $V(R)$ itself is.

5.1 Reconstruction of the continuum force

We start from a parametrization of our data on the $q\bar{q}$ -potential which has been invented by Michael [26]

$$V(\mathbf{R}) = V_0 + KR - \frac{e}{R} + \frac{f}{R^2} - \delta V(\mathbf{R}) \quad , \quad \delta V(\mathbf{R}) = el \left(\left[\frac{1}{\mathbf{R}} \right] - \frac{1}{R} \right) \quad . \quad (21)$$

The self energy V_0 , the string tension K , the Coulomb coefficient e , the lattice symmetry correction-coefficient l , and f are fit parameters. l turns out to be $l \approx 0.6$ for $\beta = 6.0, 6.2, 6.4$, and 6.8 , while f increases from 0.04 at $\beta = 6.0$ up to 0.10 at $\beta = 6.8$ as it is qualitatively expected from the running of the coupling. The χ^2 values have been found

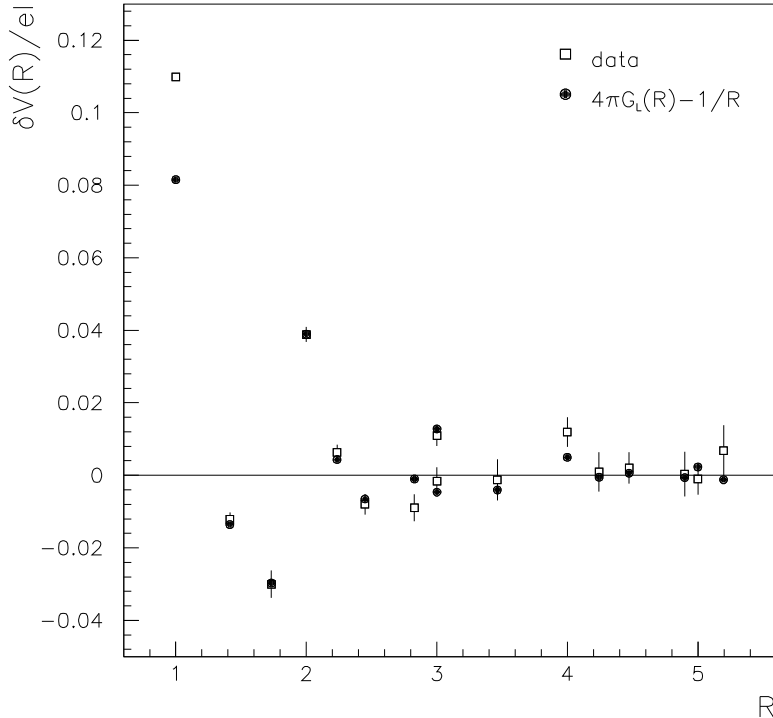


Figure 6: Comparison between deviations of the potential at $\beta = 6.4$ from the continuum symmetry $\delta V(\mathbf{R})/el$, and $[1/\mathbf{R}] - 1/R$, which has been used to parametrize lattice artefacts.

to be acceptable for the fit ranges $R \geq \sqrt{2}$ ($\beta = 6.0, \beta = 6.2$) and $R \geq \sqrt{3}$ ($\beta = 6.4, \beta = 6.8$). The quality of the fits (for the example $\beta = 6.4$) is visualized in Fig. 6 where the theoretical value $[1/\mathbf{R}] - 1/R$ (circles) is compared against $\delta V(\mathbf{R})/(el)$ (squares), as computed from the data. As a check of the stability of the parametrization we have additionally performed four parameter fits by constraining f to zero. The parameters e turned out to be smaller in these cases, while $l \approx 0.6$ was remarkably stable. Only the accepted fit ranges changed to $R \geq 2$ ($\beta = 6.0, \beta = 6.2$), and $R \geq \sqrt{5}$ ($\beta = 6.4, \beta = 6.8$), respectively.

The force can be calculated from the potential by

$$F(\overline{R}) = \frac{V(\mathbf{R}_2) - V(\mathbf{R}_1)}{2d} + \mathcal{O}\left((2d/R)^2\right) \quad (22)$$

with

$$\overline{R} = R \left(1 + \mathcal{O}\left((2d/R)^2\right)\right) \quad , \quad R = \frac{R_1 + R_2}{2} \quad , \quad d = \frac{R_1 - R_2}{2} \quad . \quad (23)$$

The smaller (larger) d is, the larger the statistical (systematic) errors become. The systematic errors stem from approximating the derivative by a finite difference. As a compromise, we have calculated the force from all pairs of potential values with distances restricted to $2 \geq 2d \geq 1$. In addition, an assumption about the smoothness of the

resulting force has been made. As an illustrative example, let us assume $V(R) = V_0 - e/R + KR$ (Eq. 6). Using the above prescription with $R_1 = R - 1$ and $R_2 = R + 1$, we obtain $F(R) = -e/(R^2 - 1) - K$. Since the expression is correct up to $\mathcal{O}(4/R^2)$ only, we can substitute $F(R)$ by $F(\bar{R})$ with $\bar{R} := \sqrt{R^2 - 1} = R(1 - 1/(2R^2) + \dots)$. This leads to the correct derivative $F(\bar{R}) = -e/\bar{R}^2 - K$. Exactly the same idea is used to calculate $\bar{R}(R, l, f/e)$ from the potential parametrization Eq. 21. This was done for $f = f_{\text{fit}}$, as well as for $f = 0$. For l a systematic error $\Delta l = l/5$ has been allowed.

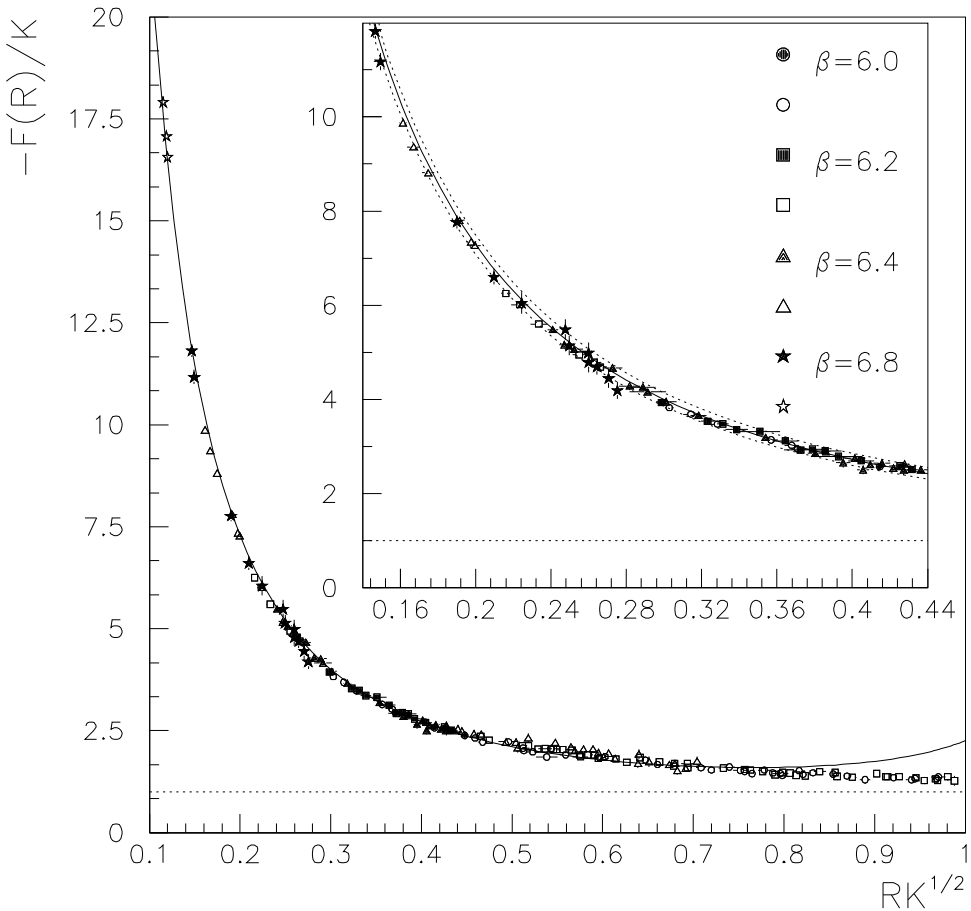


Figure 7: The reconstructed continuum force from four β -values is displayed, together with the curve $F(R) = -\frac{4}{3}\alpha_{qq}(R)/R^2$ for the parameter $\Lambda_R = 0.66(4)\sigma^{1/2}$. Horizontal errorbars denote systematic errors from taking the discrete derivative, vertical errorbars are statistical. The perturbative region is enlarged. Points with open symbols have been omitted from the determination of Λ_R .

In Fig. 7 we display the resulting continuum force for all our β -values. The systematic errors from computing the discrete derivatives are included as horizontal errorbars while the statistical errors are shown as vertical errorbars. For small R the systematic uncertainties dominate. The success of our method is illustrated by the nice scaling behaviour over the four β -values down to unexpected small distances (1.4 lattice units!).

β	R -range	$a\Lambda_R$	$\Lambda_R/\sqrt{\sigma}$
6.0	1.9–2.0	0.1440(43)	0.653(20)
6.2	1.9–2.7	0.1043(25)	0.659(16)
6.4	2.0–3.7	0.0780(24)	0.661(21)
6.8	2.0–7.0	0.0458(52)	0.656(76)

Table 2: *The plateau, in which a constant $\Lambda_R(R)$ has been observed, and the averaged Λ_R in lattice units and in units of the string tension, respectively.*

Let me finally emphasize, that the fit to Eq. 21 has just been performed to estimate the relative weight of the one-gluon-exchange $l = 0.60 \pm 0.12$. f is varied to account for systematic errors, arising from deviations from a Coulombic behaviour, due to the logarithmic running of the coupling. No additional information from the fits has been used for the numerical differentiation of the potentials.

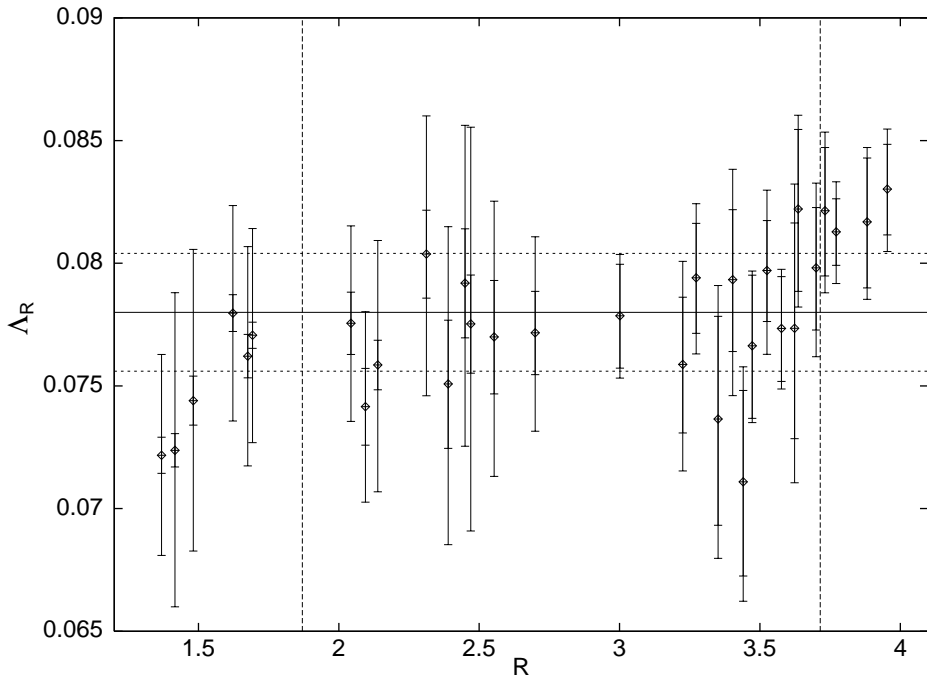


Figure 8: *The plateau in $\Lambda_R(R)$ for $\beta = 6.4$.*

5.2 Calculation of the running coupling

All data points on the force with $R_1 = 1$ are excluded from our analysis to avoid uncontrolled lattice artefacts. For all β and R values $\Lambda_R(R)$ is calculated by inverting the

relation

$$F(R) = \frac{1}{6\pi b_0} \frac{1}{R^2} \left(\ln(Ra\Lambda_R(R)) - \frac{b_1}{2b_0} \ln(-2\ln(Ra\Lambda_R(R))) \right)^{-1}, \quad (24)$$

obtained by combining Eq. 19 with Eq. 20. This ratio is plotted against R . A plateau is identified for $Ra < 1 \text{ GeV}^{-1}$ in all cases. As an example we show the $\beta = 6.4$ data in Fig. 8. The smaller errorbars indicate the statistical errors. The systematic errors are included into the larger errorbars. Below $(Ra)^{-1} \approx 1 \text{ GeV}$ the $\Lambda_R(R)$ values increase a bit, and below about 0.5 GeV the values decrease towards zero. Since the data on the force is correlated, and systematic and statistical errors cannot clearly be disentangled, we do not attempt to fit the force but average the $\Lambda_R(R)$ values over the plateau. The results are shown in Tab. 2. At $\beta = 6.4$, where $\Lambda_R(R)$ remains constant over a change of a factor *two* in the energy scale, and at $\beta = 6.8$, where this factor is about *four*, these plateaus can clearly be identified. The 6.0 and 6.2 data yield consistent but less compelling results. So, we do not attempt to use them in our final analysis. Averaging the $\beta = 6.4$ and $\beta = 6.8$ results, and allowing an additional 5% systematic error on Λ , mainly caused by the one-loop lattice artefacts (Eq. 18), leads to

$$\Lambda_R = (0.660 \pm 0.40)\sqrt{\sigma} \quad . \quad (25)$$

The corresponding fit curve is plotted in Fig. 7. As can be seen, the data is well described, even for data points that had been omitted from the Λ -determination, in order to exclude discretization errors. On the other end, the data is in qualitative agreement with the perturbative prediction down to 0.5 GeV , surprisingly close to the pole Λ_R .

The above value can be converted into

$$\Lambda_{\overline{MS}}^{(0)} = (0.630 \pm 0.38)\sqrt{\sigma} = (293 \pm 18^{+25}_{-63})\text{MeV} \quad , \quad (26)$$

using the scale estimate Eq. 9. The second error is the overall scale error from the experimental uncertainty in $\sqrt{\sigma}$. The four $\Lambda_{\overline{MS}}$ values, extracted from the force at the different β -values, as well as our final, averaged result (dashed errorband) are displayed in Fig. 4. The values scale so well that one might wonder whether we have overestimated the systematic errors. This question cannot be answered unless one-loop perturbative results on the off-axis potential are available. In Fig. 9, a comparison of the integrated perturbative force ($\Lambda_R = 0.66\sqrt{\sigma}$) with the original, uncorrected potential is made. As can be seen, the data is described quite well, even without any lattice artefact corrections. Apparently, the theoretical curve has not been biased through the analysis procedure.

5.3 Inclusion of dynamical quark flavours

How can we relate our result, $\alpha_{\overline{MS}}$ for the case of zero fermion flavours, to the real world that includes sea quarks? It is shown that our method works in principle and can be applied to dynamical configurations. In the meantime, it is possible to estimate the impact of dynamical quark flavours on the coupling by exploiting other lattice results.

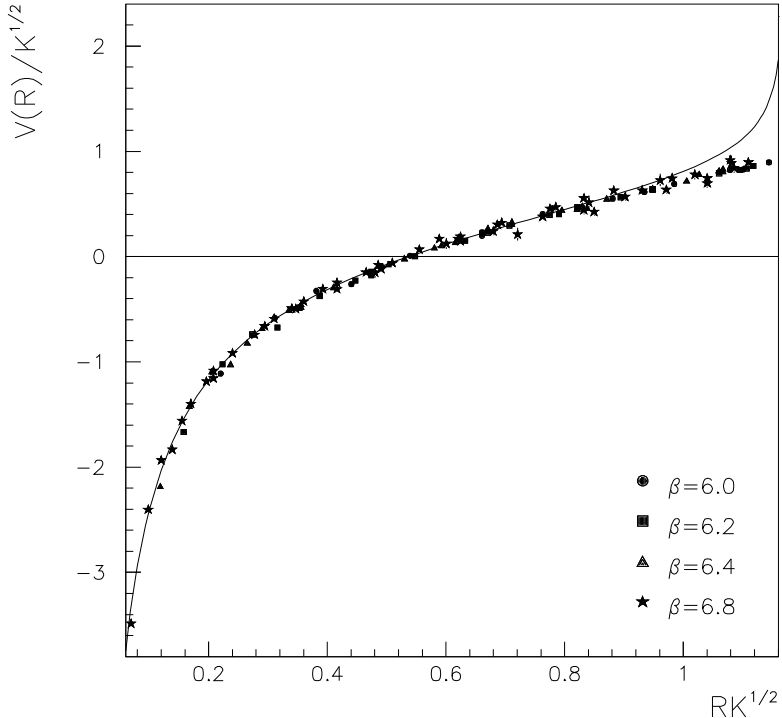


Figure 9: The uncorrected lattice potential in units of the string tension, together with the integrated perturbative force (solid curve) for $\Lambda_R = 0.66\sigma^{1/2}$.

Pioneering studies of full QCD have revealed that the sea quarks lead to a decrease of the lattice spacing a at fixed β . However, dimensionless ratios of physical observables are in qualitative agreement with quenched results. The shift in β , necessary to match a quenched lattice spacing a to the unquenched a , is called β -shift. In the following, this β -shift will be utilized to predict the corresponding change in the running coupling. From this matching, a large uncertainty in the energy scale arises but, since the coupling is running logarithmically, this has only a limited impact on the coupling at high energies, e.g. at the Z^0 mass m_Z .

For our extrapolation of $\alpha_{\overline{MS}}$ to m_Z , we use results, obtained by the MT_C collaboration [29], for four flavours of staggered quarks with a physical mass of about 35 MeV. In

$\beta^{(4)}$	$\beta^{(0)}$	$S_{\square}^{(4)}$	$S_{\square}^{(0)}$	$g_{\text{FNAL}}^{(4)}{}^2$	$g_{\text{FNAL}}^{(0)}{}^2$	$\pi/a\sqrt{\sigma}$
5.15	5.74(9)	0.4760(1)	0.443	2.0597(4)	1.79(3)	$8.5_{-1.6}^{+2.0}$
5.35	5.90(3)	0.4470(1)	0.418	1.8910(4)	1.676(9)	$12.5_{-0.9}^{+0.5}$

Table 3: Matching between four flavour QCD and the quenched approximation by use of the interquark potential. The data in the first three columns is taken from Ref. [29]. In the last column, the matching scale has been calculated.

this reference, the β -shift has been computed by matching the dynamical $q\bar{q}$ potential to the static potential. The results are collected in Tab. 3. In column *two* the corresponding quenched β values are displayed. In columns *three* and *four* the plaquette values are collected. In columns *five* and *six* g^2 has been calculated in the FNAL- \overline{MS} -scheme. In the last column, the matching momenta π/a in units of the string tension from our analysis are displayed. They are comfortably within the perturbative region. A matching between the four fermion running coupling and the quenched coupling is done, yielding $\Lambda_{\overline{MS}}^{(4)} = (0.44 \pm 0.10)\Lambda_{\overline{MS}}^{(0)}$. The scale π/a cancels from this ratio. The error consists of a 12% part from the matching of both couplings at different π/a , and a further 10% from possible scaling violations⁴, which might behave differently in the case of dynamical flavours (compared to the quenched case).

Real nature has non-degenerate quark flavours. Thus, we have to incorporate systematic errors emanating from the use of $m_u = m_d = m_s = m_c = 35$ MeV into our prediction. What is the effect of shifting m_c up to 1 GeV? If we evolve the coupling from 1 GeV down to 0.5 GeV, an energy, where perturbation theory at least qualitatively describes the running of $\alpha_{q\bar{q}}$, by use of the four flavour β -function, evolve it back with the three flavour β -function, and match it to the four flavour formula again (at 1 GeV), we find a decrease of $\Lambda_{\overline{MS}}^{(0)}$ by 10%. A shift into the opposite direction of approximately the same magnitude [30] is caused by the fact that the light quarks have been too heavy on the lattice. So, we do not intend to change our central value but increase the systematic error and end up with

$$\Lambda_{\overline{MS}}^{(4)} = 0.44_{-14}^{+10}\Lambda_{\overline{MS}}^{(0)} = (129 \pm 8_{-60}^{+43})\text{MeV} \quad . \quad (27)$$

This can be converted into a value for five flavours with an additional error from matching the couplings at $0.75m_b < \mu < 2m_b$ with $m_b = 4.8$ GeV. The final result for five active quark flavours is

$$\alpha_{\overline{MS}}(m_Z)_{-60\%}^{+45\%} = 0.102 \quad (28)$$

or, converting the scale error into an error on $\alpha_{\overline{MS}}$, this value is

$$\alpha_{\overline{MS}}(m_Z) = 0.1020_{-104}^{+054} \quad . \quad (29)$$

Even, if we assume the extreme case $\Lambda_{\overline{MS}}^{(4)} = \Lambda_{\overline{MS}}^{(0)}$, it is impossible to obtain values $\alpha_{\overline{MS}}(m_Z) > 0.115$ from the lattice. However, the effects of dynamical fermions, as well as the exact influence of quark masses [31], have to be investigated carefully in the future.

6 Summary and Outlook

With a medium scale supercomputer simulation of the valence quark approximation of QCD, a running of the strong coupling ‘‘constant’’, as predicted by perturbation theory, has been found in the region between 1 GeV and 5 GeV. Qualitative agreement with a

⁴As can be seen from Fig. 4, $\sqrt{\sigma}/\Lambda_{\overline{MS}}$, computed in the FNAL- \overline{MS} -scheme, still differs by about 25% from its asymptotic value at $a > 0.1$ fm $\approx 0.25\sigma^{-1/2}$.

Source of uncertainty	present error	future error	solution
Λ_R	3%	< 3%	smaller a , higher statistics
$\Lambda_R = \Lambda_R(R)$	5%	0%	one-loop off-axis potential
$\sqrt{\sigma} = ?$	15%	< 5%	dynamical fermions
$\Lambda_{\overline{MS}}^{(0)} \rightarrow \Lambda_{\overline{MS}}^{(4)}$	25%	< 5%	dynamical fermions
$\Lambda_{\overline{MS}}^{(4)} \rightarrow \Lambda_{\overline{MS}}^{(5)}$	2%	2%	—

Table 4: *Error sources in the calculation of $\Lambda_{\overline{MS}}^{(5)}$, and how these uncertainties can be removed/reduced.*

two-loop running was observed down to energies of about 0.5 GeV. From this, the QCD Λ -parameter (or alternatively the coupling at a given high energy scale) can be related to low energy observables like the hadron spectrum. Since the renormalization scheme in which the coupling was “measured”, is very close to the \overline{MS} -scheme, it is likely that the latter scheme gives reliable results down to energies as low as 1 GeV. Alternatively, one can use the lattice to define a renormalization scheme in a nonperturbative gauge-invariant fashion, e.g. the coupling from the interquark force.

Combining the result with phenomenological potential models [23] or data from lattice simulations of full QCD, a real world value can be estimated. The systematic part of the error, mainly caused by neglecting quark loops in the simulation, is dominant. An upper limit for $\alpha_{\overline{MS}}(m_Z)$ is found: $\alpha_{\overline{MS}}(m_Z) < 0.115$. In Tab. 4, sources of the scale errors, and how they might be removed in the near future, are collected. It should be noted, however, that, despite all systematic uncertainties, the accuracy of lattice simulations can compete with present day experiments.

The method can immediately be applied to full (lattice) QCD. The computational effort of the present investigation has been moderate, compared to most other lattice studies of quantities of direct experimental relevance. So, an analogous computation of the $q\bar{q}$ potential with dynamical fermions will become feasible in the near future. It should be amongst the earliest experiments on the first generation of TeraFLOPS computers. It will be very interesting to study the dependence of the running of α_S on the opening of new quark flavours. The impact of the quark masses and the transition behaviour at flavour thresholds can also be investigated.

Acknowledgements

I would like to thank Klaus Schilling for carefully proofreading the manuscript, and for his helpful comments and suggestions. Edwin Laermann is thanked for discussions and for letting me know the plaquette values of the MT_C simulations. The computations have been performed on the 8K Connection Machine CM-2 of the Institut für Angewandte Informatik, Wuppertal. I am grateful to Peer Ueberholz and Randy Flesch for their commitment to the Wuppertal CM project and for constant help and advice. The CM project has been supported by the DFG (grant Schi 257/1-4). This research has been funded by the EC grant # SC1*-CT91-0642.

References

- [1] F. Butler, H. Chen, J. Sexton, A. Vaccarino, and D. Weingarten, *Phys. Rev. Lett.* **70** (1993) 2849.
- [2] G.S. Bali and K. Schilling, *Phys. Rev.* **D46** (1992) 2636.
- [3] C. Michael and S. Perantonis, *Nucl. Phys.* **B347** (1990) 864.
- [4] G.S. Bali and K. Schilling, *Phys. Rev.* **D47** (1993) 661.
- [5] K. Schilling and G.S. Bali, Wuppertal preprint WUB 93-33 (1993), talk by K. Schilling at the Workshop on Large Scale Computational Physics, HLRZ Jülich.
- [6] G.S. Bali and K. Schilling, in preparation.
- [7] E. Eichten and K. Gottfried, *Phys. Lett.* **66B** (1977) 286.
- [8] C. Quigg and J.L. Rosner, *Phys. Rept.* **56C** (1979) 167.
- [9] E. Eichten, K. Gottfried, T. Kinoshita, K.D. Lane, and T.M. Yan, *Phys. Rev.* **D21** (1980) 203.
- [10] R. Sommer, DESY preprint DESY-93-062 (1993).
- [11] UKQCD Collaboration: G.S. Bali, A. Hulsebos, A.C. Irving, C. Michael, P.W. Stephenson, and K. Schilling, *Phys. Lett.* **B309** (1993) 378.
- [12] G.P. Lepage and P.B. Mackenzie, *Nucl. Phys.* **B**[Proc. Suppl.]**20** (1991) 173.
- [13] G. Parisi, Proceedings of the XXth International Conference on High Energy Physics 1980, Madison, Eds. L. Durand, and L.G. Pondrom, American Institute of Physics, New York (1981) 1531.
- [14] A.X. El-Khadra, G. Hockney, A.S. Kronfeld, and P.B. Mackenzie, *Phys. Rev. Lett.* **69** (1992) 729; P.B. Mackenzie, *Nucl. Phys.* **B**[Proc. Suppl.]**26** (1992) 369.
- [15] G.P. Lepage and P.B. Mackenzie, *Phys. Rev.* **D48** (1993) 2250.

- [16] R. Dashen and D.J. Gross, *Phys. Rev.* **D23** (1981) 2340.
- [17] A. and P. Hasenfratz, *Phys. Lett.* **93B** (1980) 165; *Nucl. Phys.* **B193** (1981) 210.
- [18] A. DiGiacomo and G.C. Rossi, *Phys. Lett.* **100B** (1981) 481; A. DiGiacomo and G. Paffati, *Phys. Lett.* **108B** (1982) 327.
- [19] U. Heller and F. Karsch, *Nucl. Phys.* **B251** (1985) 254.
- [20] B. Alles, M. Campostrini, A. Feo, and H. Panagopoulos, PISA preprint IFUP-TH-17-93 (1993).
- [21] F. Karsch and R. Petronzio, *Phys. Lett.* **153B** (1985) 87.
- [22] G.S. Bali and K. Schilling, *Nucl. Phys.* **B**[Proc. Suppl.]**30** (1993) 513.
- [23] A.X. El-Khadra, G.M. Hockney, A.S. Kronfeld, and P.B. Mackenzie, Proceedings of the 26th International Conference on High Energy Physics, Dallas (1992) 1523; A.X. El-Khadra, talk presented at the Lattice '93 conference, Dallas.
- [24] M. Lüscher, R. Narayanan, P. Weisz, and U. Wolff, *Nucl. Phys.* **B384** (1992) 168.
- [25] M. Lüscher, R. Sommer, U. Wolff, and P. Weisz, *Nucl. Phys.* **B389** (1993) 247; DESY preprint DESY-93-114 (1993).
- [26] C. Michael, *Phys. Lett.* **B283** (1992) 103; UKQCD Collaboration: S.P. Booth, K.C. Bowler, D.S. Henty, R.D. Kenway, B.J. Pendleton, D.G. Richards, A.D. Simpson, A.C. Irving, A. McKerrell, C. Michael, P.W. Stephenson, M. Teper, and K. Decker, *Phys. Lett.* **B275** (1992) 424; UKQCD Collaboration: S.P. Booth, D.S. Henty, A. Hulsebos, A.C. Irving, C. Michael, and P.W. Stephenson, *Phys. Lett.* **B294** (1992) 385.
- [27] C.B. Lang and C. Rebbi, *Phys. Lett.* **115B** (1982) 137.
- [28] A. Billoire, *Phys. Lett.* **104B** (1981) 472.
- [29] MT_C Collaboration: K.D. Born, R. Altmeyer, W. Ibes, E. Laermann, R. Sommer, T.F. Walsh, and P. Zerwas, *Nucl. Phys.* **B**[Proc. Suppl.]**20** (1991) 394; E. Laermann, private communication.
- [30] A. Hasenfratz, T.A. DeGrand, Colorado preprint COLO-HEP-311 (1993).
- [31] D.V. Shirkov, *Theor. Math. Phys.* **93** (1992) 1403.

This figure "fig1-1.png" is available in "png" format from:

<http://arxiv.org/ps/hep-lat/9311009v1>

This figure "fig1-2.png" is available in "png" format from:

<http://arxiv.org/ps/hep-lat/9311009v1>